

# INVESTIGATION OF LAMINAR NATURAL CONVECTION HEAT TRANSFER INSIDE U-SHAPED ENCLOSURE <sup>+</sup>

Khudheyer S. Mushatet \*

Qasim S. Mehdi \*\*

Abdullah K. Equabe \*\*\*

## Abstract :

In this study, the problem of steady laminar natural convection heat transfer and fluid flow inside U-shaped enclosure has been analyzed numerically. The U-shaped enclosure was differentially heated. The problem was investigated for multiple Rayleigh numbers ( $10^2 \leq Ra \leq 10^6$ ) and aspect ratios ( $0.25 \leq A \leq 0.5$ ). The mathematical model of the considered problem is formulated in terms of fully elliptic Navier-Stokes and energy equations. A numerical solution based finite volume approach is obtained. A documented results are introduced in terms of contours maps of streamlines and temperatures. Also the results are presented in terms of local and average Nusselt numbers. The results show that the aspect ratio has a significant effect on the induced multi cellular flow for high Rayleigh numbers. Also the results show that the rate of heat transfer is increased with the increase of Rayleigh number and decrease with increasing of the aspect ratio(A).

## المستخلص:

في هذه الدراسة تم اجراء الحل العددي لمشكلة انتقال الحرارة بالحمل الحر الطبقي وجريان المائع داخل حيز على شكل حرف U- علما أن الحيز مسخن تسخيناً جزئياً. أجريت الدراسة الحالية لأرقام رايلى متعددة ( $10^2 \leq Ra \leq 10^6$ ) ولنسب باعية مختلفة ( $0.25 \leq A \leq 0.5$ ). تمت صياغة النموذج الرياضي المستخدم لتحليل المسألة المدروسة بدلالة معادلات نافير و ستوكس ومعادلة الطاقة بينما تم الحصول على الحل العددي باستخدام طريقة الحجم المحدد. النتائج الموثقة في هذه الدراسة تم استعراضها على شكل خرائط كنتورية لخطوط الأنسياب ودرجات الحرارة. أيضاً قدمت النتائج التي تم الحصول عليها بدلالة أعداد نسلت الموضعية والمتوسطة. بينت النتائج التي تم الحصول عليها أن هناك تأثير واضح للنسبة الباعية على تشكيل وتكوين الجريان متعدد الدوامات ولأرقام رايلى العالية. أيضاً بينت النتائج أن معدل انتقال الحرارة يزداد مع زيادة عدد رايلى ويقل مع زيادة النسبة الباعية (A).

**Keyword: U-Shaped Enclosure, Natural Convection, Laminar**

<sup>+</sup> Received on 12/3/2009 ,Accepted on 7/12/2009 .

\* Assit prof. College of Engineering – Thi-qar University

\*\* Assit prof. College of Engineering – University of Mustansiriya

\*\*\* Assit Lect College of Engineering . Thi-qar University

## Nomenclature

A	aspect ratio (w/H), -
g	gravitational acceleration, m/s <sup>2</sup>
H	height of the enclosure, m
L	length of the enclosure, m
Nu	local Nusselt number, -
Nuav	average Nusselt number, -
n	unit normal vector, -
Pr	Prandtl number, -
Ra	Rayleigh number $\left(\frac{g\beta H^3(T_H - T_C)}{\alpha\mu}\right)$ , -
w	the distance between two walls, m
T <sub>C</sub>	cold wall temperature, °C
T <sub>H</sub>	hot wall temperature, °C
x, y	Cartesian coordinates, m
X, Y	dimensionless Cartesian coordinates (x, y)/H, -

## **Greek symbols:**

$\theta$	dimensionless temperature $\left(\frac{T - T_c}{T_h - T_c}\right)$ , -
$\alpha$	thermal diffusivity of fluid, m <sup>2</sup> /s
S <sub>φ</sub>	source term, -
Γ <sub>φ</sub>	exchange coefficients, Kg/m.s
μ	dynamic viscosity, N.s/m <sup>2</sup>
Φ	constant property, -

## Introduction:

Natural convection heat transfer and fluid flow in an enclosed enclosures acquired considerable research area due to its practical engineering applications such as cooling of electronic devices, solar collectors, double wall thermal insulation and under ground cable systems. There is a fair amount of studies on natural convection heat transfer inside enclosed enclosure but to the information of the researcher, there is shortage in studies of natural convection in U-shaped enclosure. Natural convection from differentially heated enclosures over arrange of Rayleigh numbers have received noticeable attention for many years. John[1] and Saitoh[2] investigated the 2D steady natural convection in a square cavity. They considered the effect of aspect ratio and Ra on the thermal and flow field characteristics.

Ostrach [3] analyzed numerically the natural convection in an enclosed enclosure. He made a review on natural convection heat transfer and examined different boundary conditions. Vierendeels et al.[4, 5] considered a multi grid approach to obtain the solution of incompressible fluid in an enclosed cavity for a range of Rayleigh numbers up to  $10^7$ . A conjugate heat transfer by natural convection and conduction in an enclosure was solved by Bilgen [6]. Also the laminar natural convection in enclosures was studied by Kuper[7], Marakatos [8], Rahman and Sharif [9] for different boundary conditions and orientations. Ben and Bilgen [10] studied the natural convection in an inclined enclosures bounded by a solid wall. The studied Ra was ranging from  $10^3$  to  $10^6$  and the aspect ratio from 0.5 to 1. In the present work, a numerical study is performed to analysis of the laminar natural convection in U-shaped enclosure as shown in Fig.1. The working fluid was air and the Prandtl number was fixed to 0.72. Different values of aspect ratio (0.25, 0.35, 0.5 ) and Ra ( $10^2$ ,  $10^3$ ,  $10^4$ ,  $10^5$ ,  $10^6$  ) are examined . As shown in Fig.1, the U-shaped enclosure is differentially heated and the left and bottom walls have higher temperature than the opposite internal walls. A part of the horizontal upper walls is insulated. Because of symmetry one section has been considered. The predicted results are represented in the form of stream lines and isotherm plots besides to the graphs of variation of local and average Nusselt number.

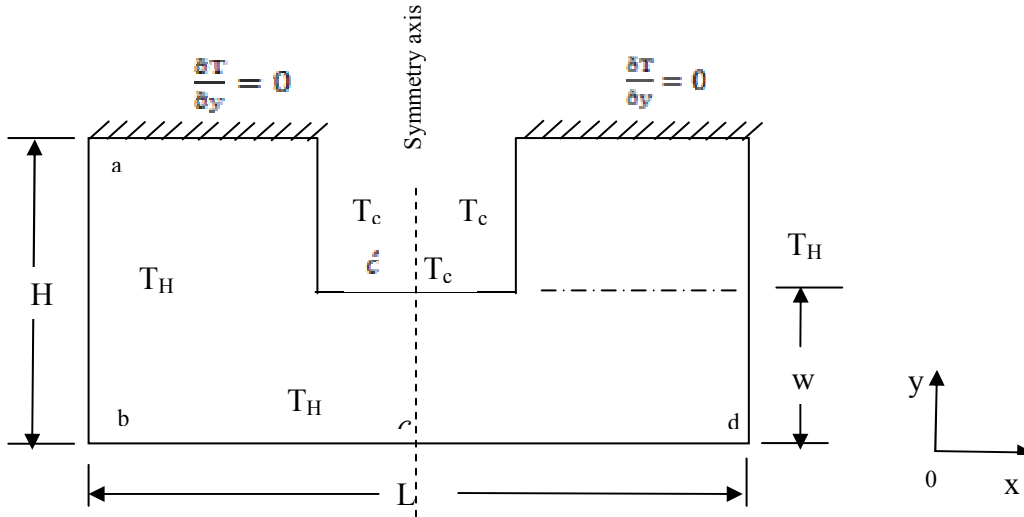


Fig.1 Problem under consideration

**Mathematical Model:**

The fluid is assumed to be incompressible , Newtonian and has a constant properties except the density in the buoyancy term of the momentum equations. The governing equations describing the considered problem can be described in dimensionless form as follows.

$$\frac{\partial}{\partial X}(U) + \frac{\partial}{\partial Y}(V) = 0 \tag{1}$$

$$\frac{\partial}{\partial X}(U^2) + \frac{\partial}{\partial Y}(UV) = -\frac{\partial P}{\partial X} + \text{Pr} \left( \frac{\partial^2 U}{\partial X^2} + \frac{\partial^2 U}{\partial Y^2} \right) \tag{2}$$

$$\frac{\partial}{\partial X}(UV) + \frac{\partial}{\partial Y}(V^2) = -\frac{\partial P}{\partial Y} + \text{Pr} \left( \frac{\partial^2 V}{\partial X^2} + \frac{\partial^2 V}{\partial Y^2} \right) + \text{Pr} Ra \theta \quad (3)$$

$$\frac{\partial}{\partial X}(U\theta) + \frac{\partial}{\partial Y}(V\theta) = \left( \frac{\partial^2 \theta}{\partial X^2} + \frac{\partial^2 \theta}{\partial Y^2} \right) \quad (4)$$

The variables under consideration can be cast in the following form:

$$X = \frac{x}{H}, \quad Y = \frac{y}{H}, \quad U = \frac{uH}{\alpha}, \quad V = \frac{vH}{\alpha}, \quad P = \frac{pH^2}{\rho\alpha^2}, \quad \theta = \frac{T - T_C}{T_H - T_C},$$

$$Ra = \frac{g\beta(T_H - T_C)H^3}{\alpha\nu}, \quad \text{Pr} = \frac{\nu}{\alpha}$$

The dimensionless stream function ( $\psi$ ) is obtained by solving the following Poisson equation with the boundary condition  $\psi = 0$  at all the solid walls:

$$\frac{\partial^2 \psi}{\partial^2 X} + \frac{\partial^2 \psi}{\partial^2 Y} = \frac{\partial U}{\partial Y} + \frac{\partial V}{\partial X} \quad (5)$$

## 1 Boundary Conditions

To complete the solution of the mentioned mathematical model, the following boundary conditions are used.

- No slip boundary conditions is imposed on the walls ( $U = V = 0$ ).
- At the symmetry axis,  $\frac{\partial \Phi}{\partial n} = 0$
- on the hot walls,  $\theta = 1$
- on the cold walls,  $\theta = 0$
- on the insulated walls,  $\frac{\partial \theta}{\partial Y} = 0$
- the local Nusselt number on the vertical left hot wall is  $Nu = \int_0^1 \frac{d\theta}{dX} = 0$
- the local Nusselt number on the horizontal left hot wall is  $Nu = \int_0^1 \frac{d\theta}{dY} = 0$
- The average Nusselt number on the hot walls can be obtained as:

$$Nu_{av} = \frac{1}{(H + L)} \left[ \int_0^1 \frac{d\theta}{dX} dy + \int_0^1 \frac{d\theta}{dY} dx \right]$$

## Numerical Procedure:

Finite volume method (FVM) with a staggered grid is used in the present numerical code. This provides us with a system of algebraic equations which means that the governing partial differential equations are transformed to algebraic equations. Then these algebraic are solved using line by line TDMA with SIMPLE algorithm. The essence of the discretization is to select appropriate discretization scheme (appropriate option of balance

between convective and diffusion terms through the boundary of each control volume.) The general governing differential equations takes the form[11]:

$$\text{div}(\rho U \Phi) = \text{div}(\Gamma \text{grad} \Phi) + S_{\Phi} \quad (6)$$

In this paper orthogonal grid with hybrid scheme is used. The one dimensional convective and diffusive fluxes can be expressed as follows:

$$J_x = \rho U \Phi - \Gamma \frac{\partial \Phi}{\partial x} \quad (7)$$

Then by using finite volume method the discretization of east side flux by hybrid scheme gives the form [11]:

$$\left( \rho U \Phi - \Gamma \frac{\partial \Phi}{\partial x} \right)_e = (\rho U)_e \frac{\Phi_p + \Phi_e}{2} - \Gamma_e \frac{\Phi_p + \Phi_e}{\Delta x_e} \quad (8)$$

A computer program is built using Fortran language to obtain the results of numerical procedure using SIMPLE algorithm. Non uniform staggered grids with refinements near the walls has been considered.

### **Results and Discussion:**

Figs.( 2 to 4) demonstrate the stream function distribution for different Rayleigh numbers and aspect ratios. For  $A=0.5$ , Fig.2(a, b, c) and  $10^2 \leq Ra \leq 10^4$ , there is a single counter rotating cell in the first part of the enclosure and a secondary flow at the corners near the symmetry axis. It can be seen that the stream lines distribution is independent of Ra. This is attributed to the superiority of conduction zone compared with the convection zone. When Ra increases to  $10^5$ , a second counter rotating cell arises in the second part of the enclosure. However the size of this cell is larger compared with the found in the first part. The size and location of the two counter rotating cells are changed when  $Ra = 10^6$ . As the aspect ratio increase to  $A= 0.35$ , the conduction dominant zone is extended only to  $Ra = 10^3$  as shown in Fig.3(a, b). When  $Ra = 10^4$ , a two re-circulating cells are appeared where the first cell in the first part is elongated and the second cell is smaller compared with  $A= 0.5$ ., As  $Ra = 10^5$ , there is a three re-circulating cells and the third cell is moved to form a large and strong re-circulating cell when the Ra is extended to  $10^6$ . This is attributed to dominant convection zone and the fast heat transfer rate when the aspect ratio is smaller. When  $A=0.25$ , Fig.4, the Ra has a significant effect on the stream function distribution. It can be seen here, there is a flow with multiple cells (three counter rotating cells) and the first cell found in the first part of the enclosure is elongated more than the above mentioned cases ( $A=0.5$  and  $A=0.35$ ). Here, the convection dominant zone is seemed to be stronger. The temperature distribution for different Rayleigh numbers and  $A= 0.35$  is depicted in Fig.5. As the figure shows, the heat is transferred from the hot walls to the cold walls through the working fluid (air) by convection. For  $Ra = 10^2$  to  $Ra = 10^4$ , the conduction zone seems to be dominant. For  $Ra = 10^5$  to  $Ra = 10^6$ , the thermo convective motion is started and it may be said that the convection zone is dominant. This is confirmed at Fig.8.a and Fig.9.a where the local Nusselt number is increased with the increase of Ra. As the figures show, the left hot corner exhibited the lower Nusselt number values, consequently the low rate of heat transfer. The temperature counter plot for  $A=0.35$  and for different Rayleigh numbers are shown in Fig.6. It can be observed that the same behavior is found for  $Ra = 10^2$  to  $Ra = 10^3$  while the convection dominant zone is started at  $10^4 \leq Ra$ . This is confirmed through observing the distribution of local Nusselt number on the vertical and horizontal hot wall as shown in Fig.8.b and Fig.9.b. The maximum

values of Nusselt number occurs at ( $y/H = 0.25$  and  $x/H=0.35$ ). The local Nusselt number is increased with the increase of Rayleigh number. As the aspect ratio is decreased to  $A=0.25$  as shown in Fig.7., the same behavior is found. However at  $Ra = 10^6$ , there is a large movements of the thermo-convective currents in the second part of the enclosure and that affected the location of maximum and minimum values of Nu as shown in Fig.9.c. The average Nu distribution as a function of Ra is demonstrated at Fig.10. It can be seen that the average Nu is increased with the increase of Ra and decrease of the aspect ratio (A) because when Ra increases, the buoyancy force increases and consequently increase the rate of heat transfer. Fig.11. disclosed the variation of the average Nusselt number with the aspect ratio (A) for different Rayleigh numbers. It can be seen that the Nu<sub>av</sub> is decreased with the increase of aspect ratio for  $10^2 \leq Ra \leq 10^3$ . This is changed for  $10^4 \leq Ra \leq 10^6$ . The considered codes is validated through the comparison with the published results in reference (8) as depicted in Fig.12. It can be observed that a good agreement has been obtained.

### **Conclusions:**

Numerical prediction of natural convection heat transfer and fluid flow inside U-shaped enclosure has been investigated. From the present computations, the following conclusions can be drawn:

- For a certain range of Ra ( $10^2 \leq Ra \leq 10^4$ ), the thermal and flow field are independent of Ra.
- For  $10^5 \leq Ra$ , the convection zone is dominant for all the considered aspect ratios.
- The multi-cellular flow is observed at the lower aspect ratio ( $A=0.25$ ) at high Rayleigh numbers ( $10^5 \leq Ra \leq 10^6$ ).
- The minor secondary flows found at the corners near the symmetry axis is observed only for the studied Rayleigh numbers and aspect ratios.
- The rate of heat transfer is increased with increase of Ra for all the studied aspect ratios

### **References**

1. Jones, IP., “ a Comparison problem for numerical methods in fluid dynamics”, International conference for numerical methods in thermal problems, Swansea, UK, pp338-348,1979.
2. Saitoh, Hirosek, k., “ High accuracy benchmark solutions to natural convection in a square cavity, J. of Computers and Fluids, 1989.
3. Ostrach, S., “ Natural convection in enclosure”, J. Heat Transfer Trans., ASME, 1988.
4. Vierendeels, J., merci, B., Dick, E., “ Numerical study of the natural convection heat transfer with large temperature difference”, Int. J. Numer. Methods. Heat Fluid Flow, 2001
5. Vierendeels, J., merci, B., Dick, E., “ a Multi grid method for natural convection heat transfer with large temperature difference”, Int. J. Comp. Appl. Math., 2004
6. Bilgen, DU, Z.G., “ Coupling of wall conduction with natural convection in a rectangular enclosure”, Int. J. Heat Mass Transfer, 1992

7. Kuper, R.A., Van Der Meer, C.J., Henkes, R.A., "Numerical study of laminar and turbulent natural convection in an inclined square cavity", , Int.J. Heat Mass Transfer,36,1993.
8. Markatos, N.C., Pericleous, K.A.," Laminar and turbulent natural convection in an enclosed cavity", Int. J. Heat Mass Transfer, 1984.
9. Rahman M., Sharif M. A., " Numerical study of laminar natural convection in rectangular enclosures of various aspect ratios", Numer. Heat Transfer, 2003.
10. Ben Yedder, Bilgen, E., " Laminar natural convection in inclined enclosures bounded by a solid wall", J. Heat Mass Transfer, Vol.32, 1997.
11. Versteeg, H. and Meer, W." An introduction of computational fluid dynamics", Hemisphere Publishing Corporation, United State of America, 1995.

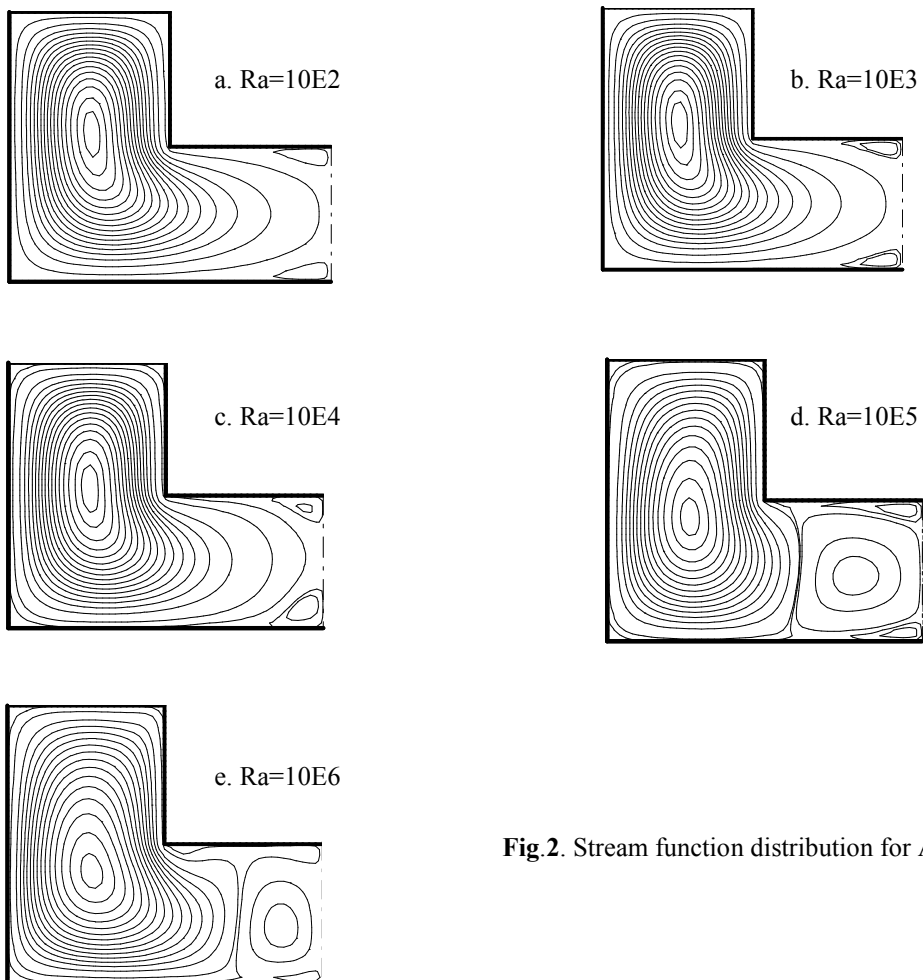
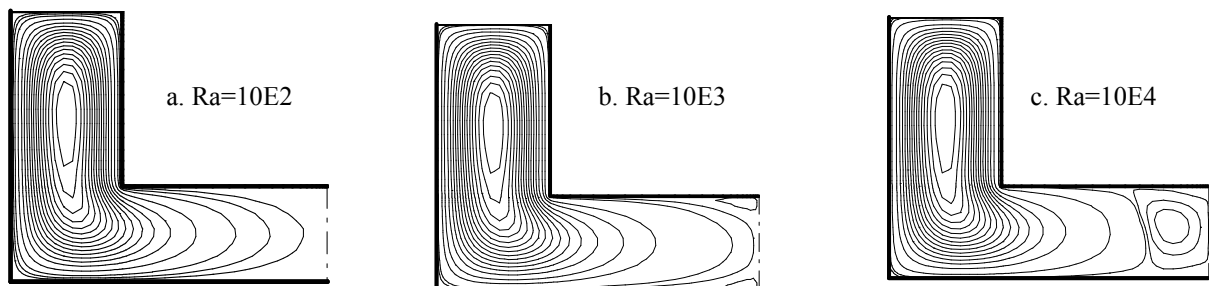
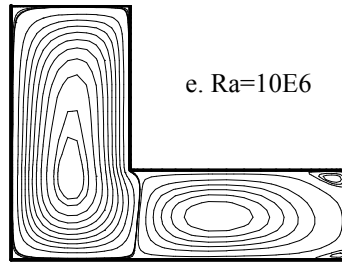
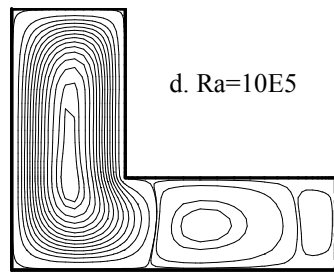
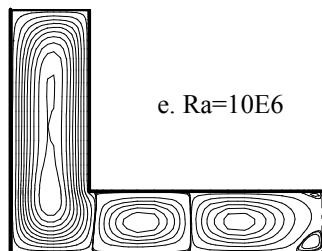
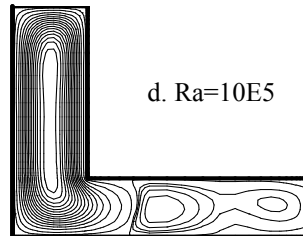
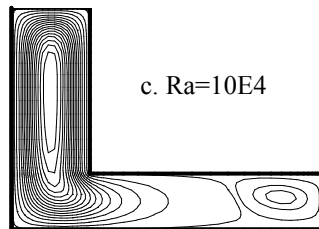
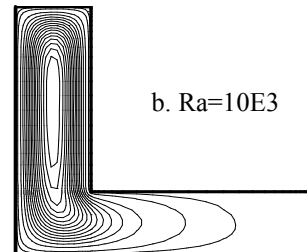
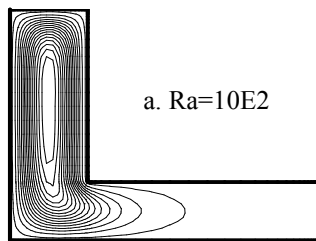


Fig 2. Stream function distribution for  $A = 0.5$

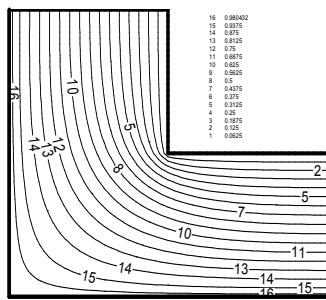




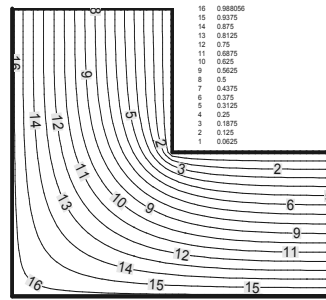
**Fig.3** Stream function distribution for  $A=0.35$



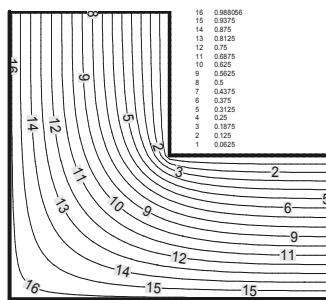
**Fig.4** Stream function distribution for  $A=0.25$



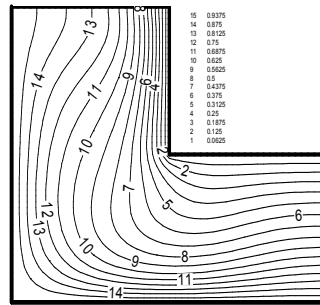
a. Ra = 10E2



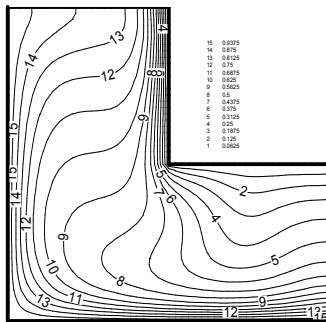
b. Ra = 10E3



c. Ra = 10E4

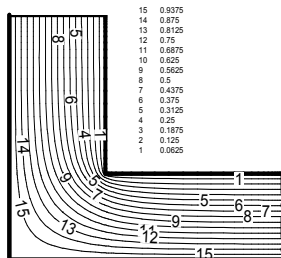


d. Ra = 10E5

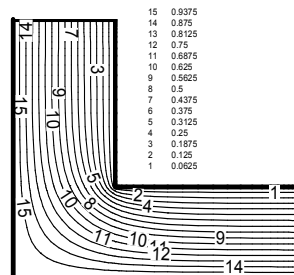


e. Ra = 10E6

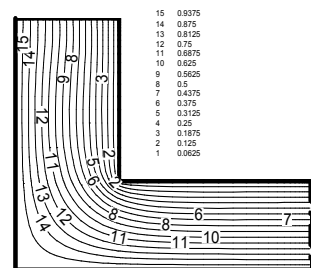
Fig.5. Isotherm contours for different Ra and A=0.5



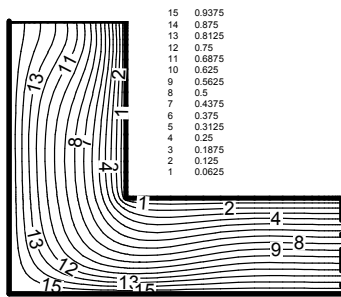
a. Ra=10E2



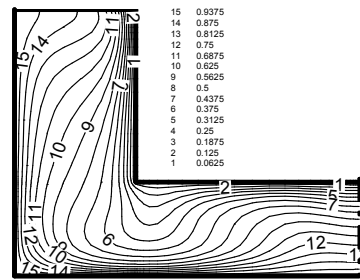
b. Ra=10E3



c. Ra=10E4

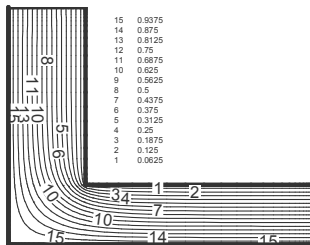


d. Ra=10E5

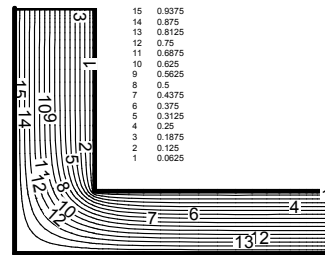


e. Ra=10E6

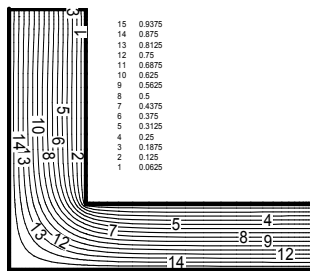
Fig.6 Isotherm contours for A=0.35



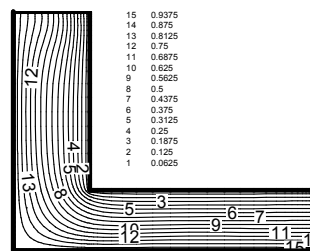
a. Ra=10E2



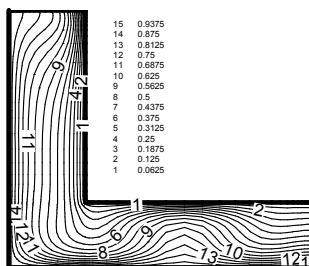
b. Ra=10E3



c. Ra=10E4

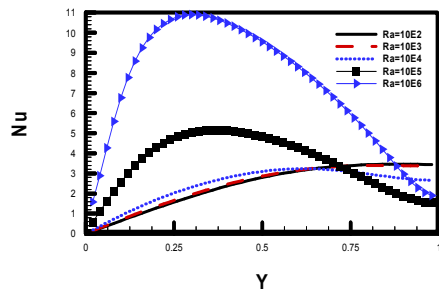


d. Ra=10E5

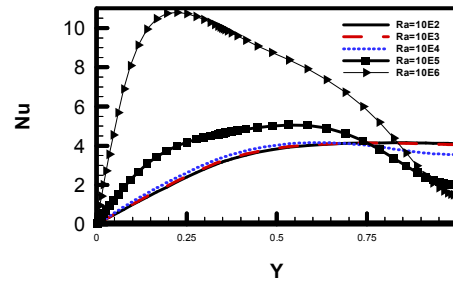


e. Ra=10E6

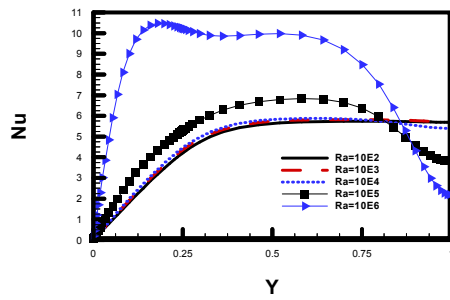
Fig.7 Isotherm contours for different Ra and A=0.25



a.  $A=0.5$

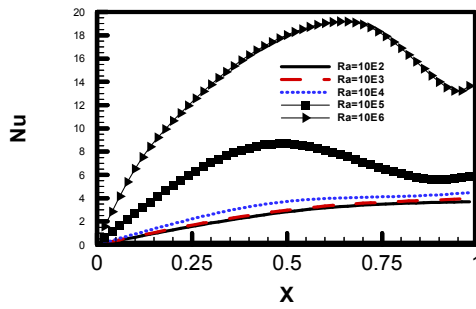


b.  $A=0.35$

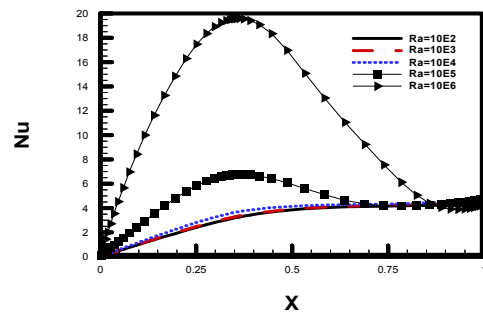


c.  $A=0.25$

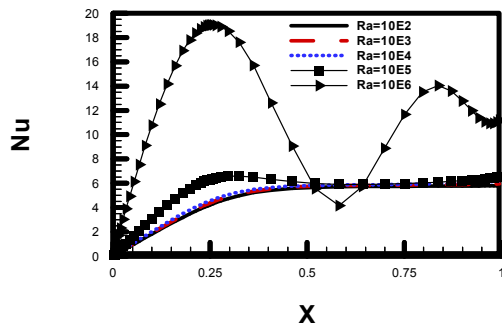
**Fig.8** Variation of local Nusselt number on the vertical hot wall for different Ra



a.  $A=0.5$



b.  $A=0.35$



c.  $A=0.25$

**Fig.9** Variation of local Nusselt number on the horizontal hot wall for different Ra

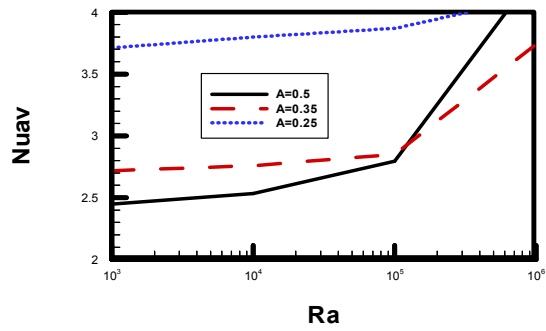


**Fig.10** Variation of average Nusselt number as a function of Ra for different aspect ratios

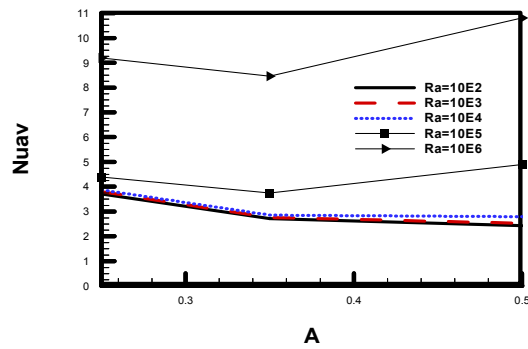
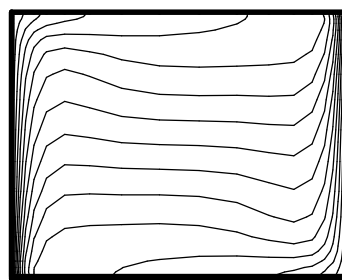
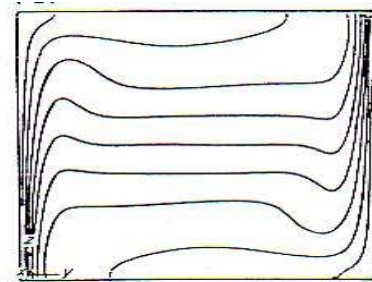


**Fig.11** Variation of average Nusselt number as a function of A for different Rayleigh numbers



a. Present results



b. Published results

**Fig. 12** Comparison between present and published results[8] for isotherm contours at Ra = 10E6